PHYSICAL REVIEW B VOLUME 38, NUMBER 16 1 DECEMBER 1988

Comparative study of secondary-electron emission from positron and electron bombardment of Ni, Si, and MgO

Rulon Mayer
Physics Department, Brookhaven National Laboratory, Upton, New York 11973

Alex Weiss
Physics Department, University of Texas, Arlington, Texas 76019
(Received 24 August 1988)

The total secondary-electron yield from positron and electron bombardment with incident energy 20–480 eV on Ni(110), Si(111), and MgO(100) has been measured. The positron-induced and electron-induced secondary-electron yield fit the same "universal" curve but with different scaling parameters. Comparison of the secondary yields suggests that the positron primary beam experiences stronger energy-loss processes than the electron beam in Ni, and qualitatively agrees with calculations and other experiments. The ratio of the maximum electron-induced secondary yield to the positron-induced secondary yield is 0.79, 1.26, and 0.6 for Ni, Si, and MgO, respectively.

Secondary-electron production through the interaction of energetic sources with materials has been extensively studied. Relatively little recent work has focused on positron-stimulated secondary-electron production.[1–4] Such an omission is unfortunate because of the renewed interest in energy-loss processes of positrons inside materials,[5,6] low-energy positron transport inside insulators,[6–8] the need to understand the positron moderation process inside ionic insulators[7] and rare-gas solids,[8] and for understanding the background in the recently observed positron-induced Auger electron emission.[9]

This paper is a comparative study of the total secondary-electron yield of the secondary electrons due to positrons and electrons with energy 20–480 eV hitting single crystals of Ni(110), Si(111), and MgO(100). The positron-induced secondary yield is qualitatively similar to that induced by electrons and is found to follow a "universal" curve. However, we find significant differences in the secondary yields for Ni, suggesting enhanced energy-loss processes and a reduced range for a positron beam relative to that of an electron primary beam. To the authors' knowledge this is the first comparison of the positron- and electron-induced yields using a direct method of normalization to the incident beam, and the first study of the positron-induced secondary yields of semiconductors and insulators under UHV conditions on well-characterized single-crystal samples.

Qualitatively, the secondary yield is an indication of the efficiency with which an incident particle exchanges energy with the electrons in the near-surface region and the ability for hot electrons to escape before losing energy. During secondary-electron production, the incident primary positrons or electrons inelastically scatter in the target, and excite electrons from the conduction band. These hot electrons can then excite other conduction electrons and may migrate back to the surface. If the electron reaches the surface before its energy drops below the electron work function of the target material, the electron can then leave the material.

The experiment was performed using a brightness-enhanced electrostatically focused beam which has been previously described.[10] The secondary-electron current was measured using a channel electron multiplier array (CEMA) equipped with a four-grid retarding-field analyzer (RFA). To reduce secondary-electron production from charged particles hitting the grids during data collection, the first grid was grounded, the second and third grids were biased to +520 V, the fourth was grounded, and the front of the CEMA was set to +500 V. The electron data were normalized by retracting the target, placing the CEMA in front of the beam, scanning the beam energy, and using the same set of voltages on the grids that were used during the data collection. The positron data were normalized by reversing the polarity on the voltage for the second and third sets of grids and the front of the CEMA. A stable low-current electron source (necessary in order to avoid saturating the CEMA) was achieved by extracting the secondary electrons produced by 2-keV positrons hitting the last remoderator (see Fig. 1 in Ref. 10). The Ni(110) crystal was cleaned by cyclically sputtering and annealing, the Si(111) crystal was cleaned by heating to 900 °C, and the MgO(100) was heated to 350 °C for 12 h. Time-dependent total yields due to charging plagued the measurements on MgO crystals, but the comparison of electrons versus positrons should still be valid. The data using MgO targets were taken under identical conditions with various target temperatures and were repeated three times.

The secondary yield δ (defined as the total electron current leaving the sample, integrated over all energies and angles, and normalized to the primary beam current) was determined from our measurements by using $\delta=[1/f(\Omega)]I(\Omega)/I_p$ where $I(\Omega)/I_p$ is the detected secondary current normalized to the incident beam and $f(\Omega)$ is the fraction of secondary electrons emitted into the solid angle of the detector. This fraction was calculat-

ed by assuming that the secondary electrons follow an experimentally observed cosine angular distribution,[1,11] and is given by integrating over the solid angle of the detector:

$$f(\Omega) = \int_{\Omega} \cos(\theta) d\Omega = 0.255 \cos(\theta_d) ,$$

where θ_d is the angle between the central axis of the detector (Fig. 1) and the normal to the sample surface (θ_d was small enough to prevent shadowing of the detector by the sample). The integrated energy distribution of secondary electrons was determined by sweeping the retarding grid of the RFA.

Figure 1(a) shows a comparison of the positron-induced and electron-induced secondary yields versus incident beam energy for Ni(110) with the incident beam hitting the surface at 78° with respect to the sample normal and with $\theta_d = 12°$. A similar comparison is shown in Figs. 1(b) and 1(c) for Si(111) and MgO(100), respectively, for the same sample and detector angles. The striking feature of these figures is the fact that while the shape of the curves is similar, the positron-induced yield is $\approx 20\%$ and $\approx 70\%$ larger than the electron-induced yield on Ni and MgO, respectively, at an incident beam energy of 480 eV, where as for Si the electron-induced yield is higher by $\approx 17\%$. Figure 1(d) shows an electron- to positron-induced yield comparison for Ni with the beam incident at 50° and $\theta_d = 40°$. Here the differences between positrons and electrons are even more pronounced. The positron-induced yield is 40% higher than the electron-induced yield at 200 eV. In addition, the positron-induced yield curve levels off well before the electron-induced curve. The solid line shown in Figs. 1(a)–1(d) represents a best fit to a "universal curve," which has been experimentally found to describe electron-induced secondary-electron emission from a large variety of metal, semiconductors, and insulators.[11] This function is given explicitly by Eq. (1):

$$\delta(E) = C_n (Z_n E / E_{0m})^{1-n} \{1 - \exp[(-Z_n E / E_{0m})^n]\} , \quad (1)$$

where E is the incident beam energy and $Z_{1.35} = 1.843$. Previous electron-induced secondary-electron-yield studies[11] have found that $n = 1.35$ yields good agreement between experiment and theory and is taken from the experimentally observed behavior of the range $R \approx E^{1.35}$. The constant E_{0m} is a scaling parameter of the universal curve and corresponds to the energy at which the secondary yield is maximum. The constant C_n is related to the maximum yield (the other scaling parameter of the universal curve) by $C_{1.35} = \delta_{\max}/0.72$. In most cases the secondary yield had not reached its maximum at 480 eV (the upper energy limit in our experimental setup), and therefore a least-squares fit to the function shown in Eq. (1) was used to determine the values of E_{0m} and $\delta_{\max}$. The values of $\delta_{\max}$ estimated from fits to the curves shown in Figs. 1(a)–1(d) are presented Table I. The values for the electron-induced secondary yield $\delta_{\max}$ from Ni and Si are in reasonable agreement with earlier values after using a procedure due to Jonker[12] to account for differences in incident polar angle (see Table I). Differences in the extrapolated values and earlier studies may be due to the failure of the extrapolation method, which has not been tested at these large incident scattering angles (78°). The electron-induced secondary-electron yield $\delta_{\max}$ from MgO is low relative to previously published reports.[13,14] The disparity in the values of $\delta_{\max}$ could be due to sample preparation and charging problems. We find the ratio of $\delta_r = \delta^-_{\max}/\delta^+_{\max}$ or the maximum electron-induced to

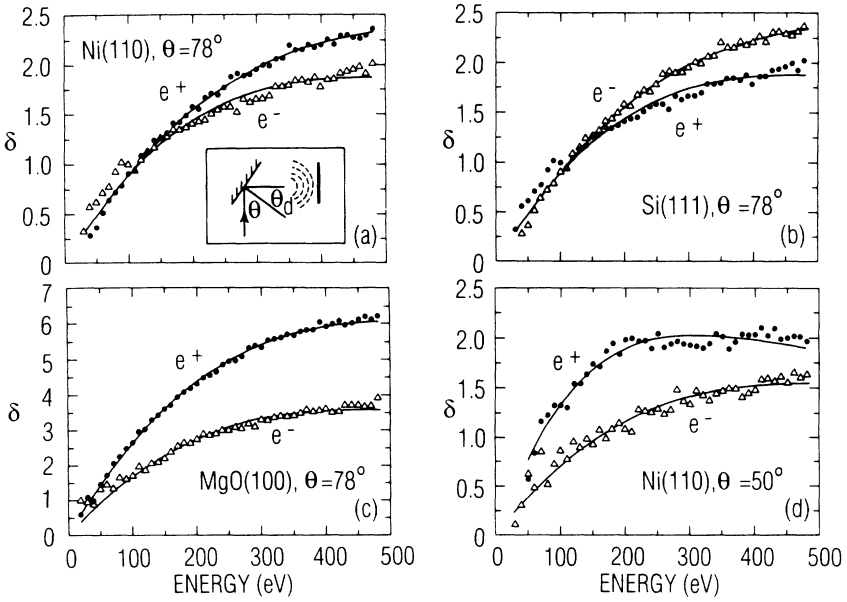

FIG. 1. (a) Comparison of the secondary-electron yields from Ni(110) due to positrons and electrons incident at 78° as a function of incident beam energy. Solid lines are functions obtained from fits to Eq. (1). Inset depicts beam, sample, detector arrangements; (b) same as (a) except target is Si(111); (c) same as (a) except target is MgO(100); (d) same as (a) except incident polar angle is 50°.

TABLE I. Values of δ_{max} estimated from Fig. 1 by using Eq. (1), $C_{1.35}=\delta_{max}/0.72$, $n=1.35$, and curves in Fig. 1.

Sample	Angle of incidence ($\mp 2°$)	e^+, e^-	δ_{max} (∓ 0.2)	δ_{max}^{11}	$\delta_{e^-}/\delta_{e^+}$
Ni(110)	50°	e^+	2.0		0.75
Ni(110)	50°	e^-	1.5	1.5[a]	
Ni(110)	78°	e^+	2.4		0.79
Ni(110)	78°	e^-	1.9	2.4[b]	
Si(111)	78°	e^+	1.5		1.26
Si(111)	78°	e^-	1.9	2.2[c]	
MgO(100)	78°	e^+	6.1		0.6[e]
MgO(100)	78°	e^-	3.6	15–50[d]	

[a]Reference 12 for $\theta=48°$.
[b]Extrapolated from $\delta_{max}=1.9$ at $\theta=70°$ (Ref. 12).
[c]Extrapolated from $\delta_{max}=1.1$ at $\theta=0°$ [L. R. Koller and J. S. Burgess, Phys. Rev. **70**, 571 (1946)].
[d]Reference 11.
[e]Reference 2.

positron-induced secondary-electron yield for the MgO sample is 0.6. This is significantly different from Cherry's[2] value of 3.

The limited energy range of the experimental data implies a large uncertainty in the fitted value of E_{0m} especially for targets whose $E_{0m} > 500$ eV. Studies of positron energy loss (for incident particles $\approx$1–6 keV), unlike electron energy loss[11] in thin films,[15] find the mean penetration depth follows E^n where $n=1.6$. Substitution of $n=1.6$ into Eq. (1) yielded a slightly worse χ^2 fit to the data relative to $n=1.35$. Due to the limited energy range of our data and the simple assumptions of Eq. (1), we cannot definitively conclude that the energy loss per distance follows $n=1.35$.

Recent calculations by Zhang, Tzoar, and Platzman,[16] low-energy positron-diffraction experiments,[17–20] and glancing-angle positron-diffraction and positronium-formation[21] studies suggest that positron energy-loss processes are greatly enhanced relative to those for electrons in metals for particles in the energy range of this experiment. This is partially due to the fact that attraction between positrons and electrons leads to increased collision rates relative to electron-electron scattering.[16] The range R of a positron primary beam therefore should be reduced relative to that of an electron beam because of the stronger inelastic scattering.

A connection between enhanced energy loss, reduced range, and the observed yields in this experiment can be obtained by using the following reasoning. In this argument, the secondary-electron escape depth λ from the two types of incident particles is assumed to be the same for a particular sample target and scattering geometry, and λ is assumed to be energy independent (evidence that λ is in fact not the same will be discussed below). A relation between δ_{max} and range R is implicit in the semiempirical Dekker theory[11] and is shown in Eq. (2),

$$\delta_{max} \approx \left[\frac{\lambda}{R_0}\right]^{1/1.35}, \quad (2)$$

where $R=R_0E^{1.35}$. Using our values of δ_{max} in Eq. (2), the positron range relative to the electron range is reduced by 70% and qualitatively agrees with the calculations of Zhang *et al.* for metals with $r_s/a_0=2$ [$r_s/a_0=2.38$ for Ni (Ref. 22)].

The differences in positron and electron energy loss in the near-surface region of Ni(110) are even larger than is indicated by the disparity in the total yields shown in Figs. 1(a) and 1(d). The electron-induced yield is enhanced in Figs. 1(a) and 1(d) due to the presence of extra "backscattered" electrons (energy >20 eV) in the electron-induced spectrum that are absent in the positron data as can be seen in Figs. 2(a) and 2(b), which show the integrated electron energy distribution [$=\int_E^\infty (dn/d\varepsilon)d\varepsilon$] due to 100-eV positrons and electrons, respectively, and was measured using the RFA of the CEMA. The integrated yield has been normalized to a common value of 100% at $E=0$ eV. The energy-independent counts from annihilation γ rays and positronium have been subtracted from the positron spectra [Fig. 2(a)].

The presence (absence) of backscattered electrons in the electron- (positron-) induced total yield not only affects δ_{max} but also E_{0m} and complicates the comparison of the spectra. Referring to Fig. 1(d), it is clear that the maximum yield from positrons is reached at a lower ener-

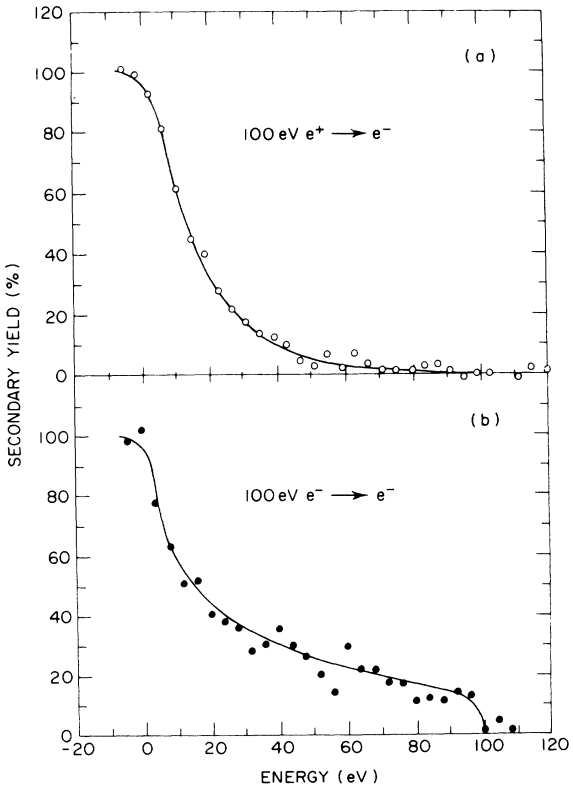

FIG. 2. (a) Normalized secondary-electron energy distribution from 100-eV positrons hitting the Ni(110) surface at 78°. Counts due to annihilation γ rays and positronium have been subtracted. The solid line is a guide for the eye; (b) same as (a) except incident beam is from 100-eV electrons. No subtraction from γ rays and positronium.

gy E_{0m} but that δ_{max} is higher for positrons than for electrons. This relationship between δ_{max} and E_{0m} is inconsistent with the semiempirical Dekker theory in which δ_{max} and E_{0m} should increase together, assuming λ is energy independent and is the same for the positron- and electron-induced secondaries. This inconsistency can be explained by noting that the presence of backscattered electrons in the electron-induced spectrum raises the average energy of the electron-induced spectrum and causes an energy dependence for the escape depth λ. Also, the dependence of the backscattered electron yield on incident beam energy[23] differs from that of low-energy secondary electrons (< 20 eV).

Presently, there is no quantitative understanding of the positron-induced secondary-electron production. A calculation using Monte Carlo methods and more extensive experimental studies of the secondary-electron angular and energy distributions may help lead to an understanding of the problem.

The work done at Brookhaven National Laboratory was supported by U.S. Department of Energy Contract No. DE-AC02-76CH0016. The work done at the University of Texas was supported by the Robert A. Welch Foundation, the Texas Advanced Technology Research Program, and the Texas Advanced Research Program.

[1]Alex Weiss, Ph.D. thesis, Brandeis University, 1982 (unpublished).

[2]W. H. Cherry, Ph.D. thesis, Princeton University, 1958 (unpublished).

[3]S. Pendyala, J. Wm. McGowan, P. M. R. Orth, and P. W. Zitzewitz, Rev. Sci. Instrum. **45**, 1347 (1974).

[4]A. Weiss and K. F. Canter, in *Proceedings of the 6th International Conference on Positron Annihilation, Texas, 1982,* edited by P. G. Coleman, S. C. Sharma, and L. M. Diana (North-Holland, Amsterdam, 1982).

[5]B. Nielsen, K. G. Lynn, and Y. C. Chen, Phys. Rev. Lett. **57**, 1789 (1986).

[6]K. G. Lynn and B. Nielsen, Phys. Rev. Lett. **58**, 18 (1987).

[7]A. P. Mills, Jr. and W. S. Crane, Phys. Rev. Lett. **53**, 2165 (1984).

[8]E. M. Gullikson and A. P. Mills, Jr., Phys. Rev. Lett. **57**, 376 (1986).

[9]A. Weiss *et al.*, in *Proceedings of VIII International Conference on Positron Annihilation,* edited by L. Dorikens-Varpraet, M. Dorikens, and D. Segers (World Scientific, Singapore, in press).

[10]W. E. Frieze, D. W. Gidley, and K. G. Lynn, Phys. Rev. B **31**, 5628 (1985).

[11]A. J. Dekker, in *Solid State Physics,* edited by F. Seitz, D. Turnbull, and H. Ehrenreich (Academic, New York, 1958), Vol. 6, pp. 251–311.

[12]J. L. H. Jonker, Philips Res. Rep. **7**, 1 (1952).

[13]J. B. Johnson and K. B. McKay, Phys. Rev. **91**, 582 (1953).

[14]R. G. Lye, Phys. Rev. **99**, 1647 (1955).

[15]A. P. Mills, Jr. and R. J. Wilson, Phys. Rev. A **26**, 490 (1982).

[16]C. Zhang, N. Tzoar, and P. M. Platzman, Phys. Rev. B **37**, 7326 (1988).

[17]R. Mayer *et al.*, Phys. Rev. B **35**, 3102 (1987).

[18]R. Mayer *et al.*, Phys. Rev. B **36**, 5659 (1987).

[19]R. Mayer *et al.*, in *Electronic and Atomic Collisions,* edited by H. B. Gilbody, W. A. Newell, F. H. Read, and A. C. H. Smith (Elsevier, New York, 1988), p. 803.

[20]A. H. Weiss *et at.*, Phys. Rev. B **27**, 867 (1983).

[21]D. W. Gidley, R. Mayer, W. E. Frieze, and K. G. Lynn, Phys. Rev. Lett. **58**, 595 (1987).

[22]J. A. Alonso and M. P. Iniguez, Solid State Commun. **33**, 59 (1980).

[23]E. H. Darlington and V. E. Cosslett, J. Phys. D **5**, 1969 (1972).